

Preparation and Evaluation of Physical/Chemical Gradient Bone Scaffold by 3D Bio-printing Technology

Yanan ZHANG^a, Yuanyuan LIU^{a,1}, Haiping CHEN^a, Zhenglong JIANG^a,
and Qingxi HU^a

^aRapid Manufacturing Engineering Center, Shanghai University, Shanghai 200444

Abstract. Bone scaffold with fully interconnected pores whose sizes are gradient structured can be prepared by 3-dimensional (3D) printing technology, and has presented important value in tissue engineering. It is known that, in the direction of bone thickness, the composition, structure and performance are continuously varied, and the number and species of related cells distributed in different regions are different. Based on biological 3D printing platform constructed adopting rotary pneumatic multi-nozzle structure and poly-L-lysine (PL) modified matrix materials, and in order to better simulate the spatial morphology of bone tissue and its function and make seed cells rapidly and accurately migrate to the specific region, a novel approach for preparing composite physical/chemical gradient bone scaffold was proposed. Dividing the scaffold into three different regions, the structure property and mechanical performance of different regions were detailedly analyzed. In addition, using adipose derived stem cells (ASCs) as seed cells, their initial adhesion on different regions and corresponding viability analysis were also conducted, respectively. The experiment results show that gradient material can make the cell migrate toward and attach on specific location and optimizing its physical structure can improve its mechanical properties. Thus the composite gradient scaffold prepared through this approach presents great potential application for in vitro constructing complex tissues and organs.

Keywords. 3D bio-printing; multi-nozzle; material modification; gradient bone scaffold; tissue engineering

Introduction

With the development of molecular biology, medicine, material science and interdisciplinary sciences, bone tissue engineering provides new ideas for treating bone injury. In this approach seed cell and scaffold are two major elements [1,2], and scaffold serve as temporary carrier, and provide biological and physical cues to support cell adhesion, proliferation and induce differentiation of stem cells for mediating cell behavior including regeneration [3,4]. The continuous gradient variation of these cues in the scaffold such as porosity, mechanical strength and the concentration of bioactive molecules can greatly affect the biological characteristics of cells [5]. Therefore, the physical structure and biochemical properties of scaffolds are extremely important in tissue repairing and regeneration processes.

¹ Corresponding author: Yuanyuan Liu. E-mail: yuanyuan_liu@shu.edu.cn.

3D printing technology is a high-tech manufacturing technique whose process is based on material accumulation and compared with traditional techniques, is less affected by the complexity of physical prototype. Scaffolds with fully interconnected pores whose sizes are gradient structured can be produced by it, and its excellent permeability and mechanical properties can meet the requirement of tissue engineering scaffolds [6-8]. Sobral et al [9] realized the preparation of 3D physical gradient bone scaffold, and the gradient of pore size greatly reduced the loss of cells, thus having improved seeding efficiency. However, bone is a complex tissue with gradients, not only in the aperture, porosity and mechanical strength, it is also an ordered structure composed of a variety of cells. Physical gradient only cannot effectively guide the seed cells to migrate orderly and in a certain direction, thus not being able to make cells adhere to and grow in specific area.

In this study, besides the physical gradient, another chemical gradient was proposed, namely the material gradient. Due to its structural similarities to the extracellular matrix (ECM) of living tissues, low toxicity and excellent biocompatibility, Sodium alginate is used as matrix material. However, its strong hydrophilic property is not conducive to the adsorption of protein and the initial adhesion of cells [10-13]. With good biocompatibility, Poly-L-lysine (PL) is widely used in bone repairing material. Lysine residues fixed on the surface of bone repair material carry positive charges, which can attract the negatively charged cells and thus improve the initial adhesion. In addition, PL can adjust the hydrophilic/hydrophobic balance of material surface by its amino group (-NH₂), and promote cells adhesion by the interaction between functional groups and protein peptide chain on the cell surface [14-16]. Therefore, PL was used to modify the matrix material. Material gradient was formed in the scaffold between not-modified and modified matrix material. After receiving these gradient cues, seed cells will selectively migrate to the target region and then start growing and proliferation [17-19]. With inducement conducted in this way, formation of a bionic bone tissue *in vitro* can be possible.

In order to obtain this composite gradient scaffold, in this research, the Biological 3D printing platform was developed. The rotary pneumatic multi-nozzle structure using compressed air as power was also constructed, which can realize accurate switching and assembly for different materials or cells. In addition, to explore the applications of this scaffold in tissue engineering, mechanical properties and porosity of the scaffold, cell initial adhesion and viability analysis were also conducted in this paper.

1. Materials and methods

1.1. Materials

Sodium alginate (Sigma, UK) was used as matrix material while PL (Sigma, UK) as the modified material. The solution of Sodium alginate with weight fraction at 4% (w/v) in deionized water was placed in a shaker for 10 h at 120 rpm, referring as Material 1 (M1). Similarly, after preparing sodium alginate, a certain amount of PL was added to the alginate solution to modify the matrix material. The modified-material was referred as Material 2 (M2).

1.2. Experimental procedures and Scaffold fabricating

The experiment was carried out on the Biological 3D printing platform (home-built equipment, Shanghai University, China), shown in Fig.1. It consisted of four main parts: a computer controlled three-axis motion mechanism, multi-nozzle structure, forming platform and variable management module. Pneumatic multi-nozzle structure using compressed air as power and circumferential arrangement, can be freely switched among four nozzles in the forming plane, presenting high degree of automation.

The model of the composite gradient scaffold was shown in Fig.2, fabricated as $25 \times 25 \times 15 \text{ mm}^3$, alternating layers were oriented at 90° to each other. The scaffold was divided into three different regions (Region A, Region B, Region C), and there were two gradients among them. Region A and Region B had the same pore size, the fiber spacing (L1) was set to $500 \mu\text{m}$, but the material of Region A was M1, the material of Region B was M2. The fiber spacing of Region C (L2) was set to $300 \mu\text{m}$, and its material was M1.

When preparing the scaffold, M1 and M2 were respectively injected into Syringe A and Syringe B, and extruded by compressed air. Process parameters were set as follows: the nozzle diameter was 0.5 mm , the feeding speed 0.4 mL/min , and the forming platform speed 12 mm/s . Region C was printed firstly, after that, alternately printed Region A and Region B. During the forming process, it needed accurate switching between the two nozzles. After the preparation of the scaffold, put it into the freeze dryer for freeze drying.

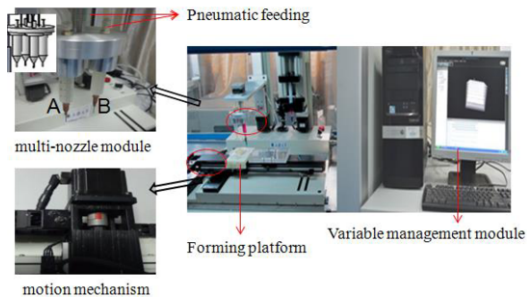


Figure 1. Biological 3D printing platform

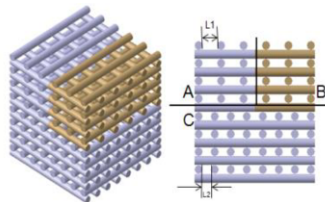


Figure 2. Schematic model of composite gradient scaffold

1.3. Scaffold characterization

1.3.1. Morphology of scaffold

The morphological characterization of scaffold was analyzed by the scanning electron microscope (SEM, SU1510, Analysis and Testing Center, Shanghai University). The samples were cut into $5 \times 5 \times 5 \text{ mm}^3$ cubes, treated with glutaraldehyde (Sigma, USA),

desiccated with ethanol, vacuum-dried, and pre-coated with a conductive layer of sputtered gold. The micrographs were taken at different magnifications.

1.3.2. Porosity of scaffold

In this study, the scaffold was divided into three different regions, so the porosity needed to be calculated respectively. The three regions were respectively sampled, each region taking five specimens. The values reported in the next section were the average of five specimens. Then the porosity (E) was measured by the Archimedes principle, calculated by the formula as follow:

$$E = \frac{V_1 - V_3}{V_2 - V_3} \times 100\%$$

where V1 denotes the initial volume of ethanol; V2 the ethanol volume after a specimen has been immersed into; V3 the ethanol volume when the specimen is removed.

1.3.3 Mechanical testing

In order to characterize the mechanical properties of scaffolds, compression tests were carried out on pressure testing machine (Instron5542, Canton, USA). Samples of the three regions were made into $5 \times 5 \times 2 \text{ mm}^3$, and were placed on the pressure testing machine, carrying the static loading test in the vertical plane at a speed of 0.5mm/min until reaching the amount of 90% compression. An average compressive modulus was determined for all samples (n=5 per group).

1.4. Cell culture and cell morphology

1.4.1. Co-culture of cell-scaffold constructs in vitro

Scaffold samples were fixed with glutaraldehyde, cleaned by deionized water, disinfected with 75% alcohol, and cleaned by phosphate-buffered saline (PBS) solution at last. In the sterile environment, the third passage ASCs (provided by Shanghai Tissue Engineering and Research Center) with good growth state were harvested by 0.25% Trypsin-EDTA (Life Technologies, NY), could finally be seeded into the samples which have been pretreated. The cell-scaffold constructs were co-cultured in an atmosphere of 5% CO₂ at 37°C in Dulbecco's Modified Eagle's Medium (DMEM) with 10% fetal bovine serum (FBS) medium. Culture medium was changed every other day.

1.4.2. Fluorescence analysis

Cells seeded on the scaffolds needed enough time to attach and adapt to the different scaffold architectures and materials, so these cell-scaffold constructs were taken out from the CO₂ incubator after seeding for 24 h. All the specimens selected for fluorescence microscopy were fixed in 4% paraformaldehyde (Sigma, USA) solution in PBS for 1 h at 4°C. After washing by PBS, all specimens were labeled by the fluorescent reactive dye DIO for 10 min, then washed three times with PBS. These specimens were observed via Inverted fluorescence microscope (IFM, IX71).

1.4.3. Cell morphology and cell attachment

The morphologies of the cells on different substrates was observed by SEM after seeding 72 h. Specimens were washed three times with PBS, fixed with 2.5% glutaraldehyde solution in PBS for 1 h at 4°C, sequentially dehydrated in increasing concentrations of ethanol (from 25, 50, 75, 80, 95 to 100%, each for 15 min), then vacuum-dried. The dried samples were coated with Au by a sputter coater and examined by SEM to determine the adhesion and ECM deposition of ASCs on the scaffold.

1.4.4. Cell proliferation assay

For cell proliferation assay, ASCs were plated at a density of 3×10^3 cells/cm² into the specimens. Cells at indicated time points (1, 3, 5, 7, 9, 11 days) were crushed and repeated freezing and thawing to release DNA. DNA quantification was performed (n=9 per group per time point) using Hoechst 33258 dye (Sigma-Aldrich) following the manufacturer's protocol.

2. Results and discussion

2.1. Scaffold characterization

As shown in Fig.3, the composite gradient scaffold was successfully produced. From the positive view of the scaffold (Fig.3a), the pore architecture of scaffold was fully interconnected and the whole structure was regular; from the side view (Fig.3b), the aperture difference, tight junction and natural transition between Layer 1 and Layer 2 can be obviously observed. Good bonding between the layers was essential for mechanical stability of the scaffolds. The fiber spacing of Layer 1 and Layer 2 was 293μm and 516μm respectively, measured by SEM. There was a slight deviation between actual value and the theoretical value, as shown in Table 1. In addition, due to the aperture gradient structure, there was an offset between Layer 1 and Layer 2, as shown in Fig.3d. Compared with scaffolds with uniform aperture, the gradient scaffold provided more tortuous conduits inside the scaffold, which could increase the residence time of cells in the scaffolds and increase the likelihood of contact between the cells and the surface of the scaffold, greatly improving the cell seeding efficiency [8].

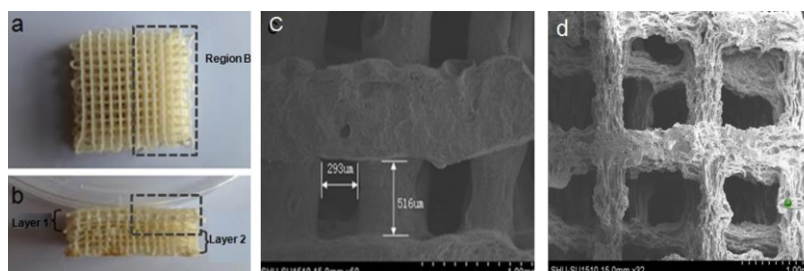


Figure 3. The composite gradient scaffold.(a) scaffold positive view;(b) scaffold side view; (c) microstructure of pore size gradient;(d) the scattered arrangement between Layer 1 and Layer 2

Bone includes two typical forms: compact bone and spongy bone. Compact bone forms the extremely hard exterior while spongy bone fills the hollow interior. From the bone’s outer layer to the inner layer, the aperture is bigger and bigger, therefore, the porosity gradient is necessary to the preparation of bionic bone, and directly affects its mechanical properties. In the scaffold, Region A and Region B had the same pore size, their porosities measured by the Archimedes method were basically the same, about 68%, as shown in Table 1, while for Region C, the total porosity was 61%. As expected, for the whole gradient scaffold the total porosity values was intermediate between 68% and 61%, about 66%.The composite gradient scaffold met the porosity change of normal bone tissue from cortical bone to the spongy bone, and met the requirements of scaffold porosity for bone tissue engineered.

Table 1.Parameters for each region of scaffold

Scaffold regional	Aperture in theory(um)	Real aperture(um)	Porosity(%)
Region A	500	500±25	68±0.5
Region B	500	500±25	68±0.5
Region C	300	300±25	61±0.3
The whole scaffold	—	—	66±0.3

Bone scaffold with good mechanical properties can simulate the micro-stress environment of living organs, contribute to cell proliferation and differentiation in the scaffold. Fig.4 showed the stress and strain curves obtained for all specimens. For Region A and Region B, had the same aperture and different materials, compression capability was almost the same when having the same compression displacement. It indicated that the modification of matrix material had little effect on the mechanical properties, however, to a certain extent, the pore size and porosity of the scaffold determined the mechanical properties. As the stress-strain curves showed, Region C with lower porosity showed stronger compressive mechanical properties, indicating the expected relationship between porosity of the scaffolds and the respective mechanical properties.

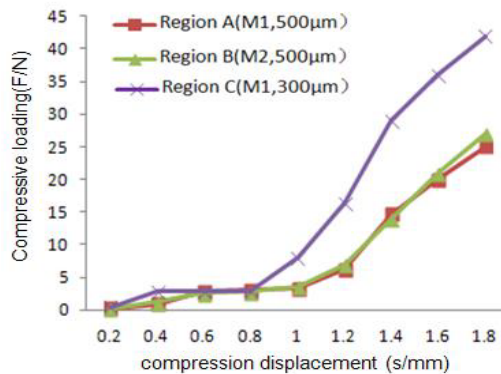


Figure 4. Stress-strain curve for each region

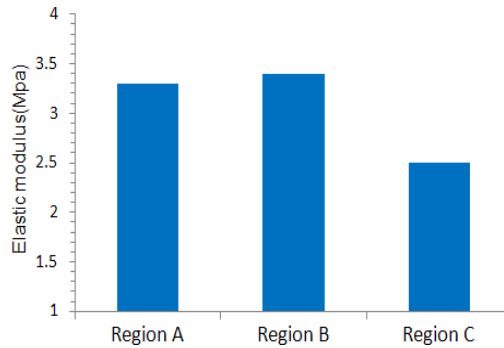


Figure 5. Elastic modulus for each region

Fig.5 showed the elastic modulus of each region: Region C with the good compressive properties exhibited low elastic modulus, while Region A and Region B exhibited higher elastic modulus. The above results showed that: there were some great relationships among pore size, porosity and mechanical properties, therefore, reasonable selection of aperture parameters and rational deployment of the gradient structure can realize the preparation of bionic bone scaffolds which not only meet the strength requirements but also suitable for cell growth.

2.2. Biological performance

To evaluate cell response to the material gradient of the scaffold, ASCs were plated at the same density in the samples and co-cultured. The cell adhesion on substrate could be regarded as the first step in culturing constructs for tissue regeneration [20]. For the studying of ASCs initial adhesion on different regions, the DIO-labeled cells were observed via IFM. As shown in Fig.6: Region B modified by PL was more attractive to ASCs than Region A. The quantity and distribution density of ASCs initial adhesion on Region B were significantly higher than those on Region A. This suggested that materials gradient, to a certain extent, instructed the ASCs to migrate to Region B, and then realized their initial adhesion and aggregation; the modification effect of PL on matrix material was obvious, significantly improved its biocompatibility.

Cell morphology and the interaction between cells and scaffold were studied after having been co-cultured for three days *in vitro*. As shown in Fig.7, some ASCs adhered on Region A were relatively small and still kept spherical, without sufficient adhesion and spreading. However, cells on Region B showed a good attachment, with fully extended, the spreading area was larger and secreted more EMC. In addition, cells still kept fibroblast-like morphology and connected with each other by pseudopodia. The results showed that, PL could promote cell adhesion, cell spreading and cell growth. With the gradient change of the scaffold material, the growth state of cells was changing.

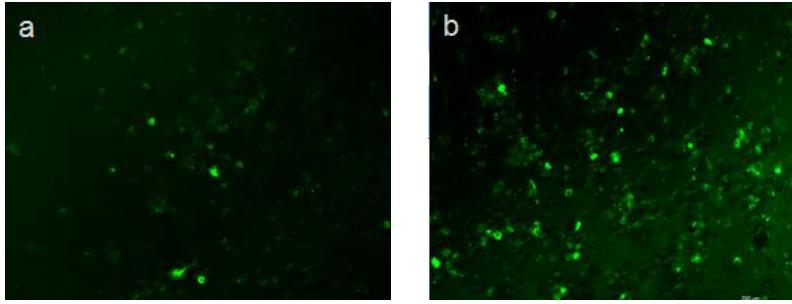


Figure 6. Initial adhesion of ASCs on different regions observed by IFM
(a) DIO-labeled ASCs on Region A; (b) DIO-labeled ASCs on Region B

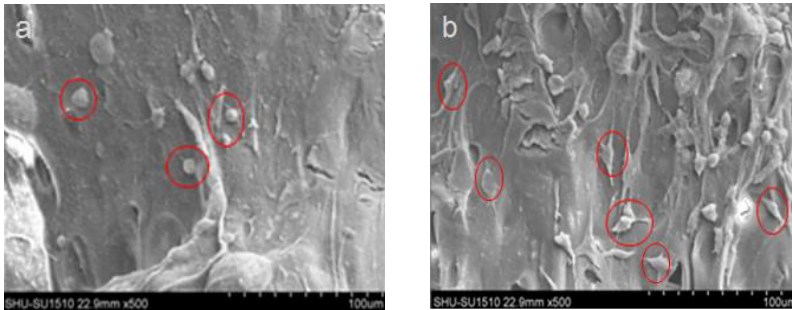


Figure 7. SEM of ASCs cultured on different regions for 3 days.
(a) ASCs on Region A; (b) ASCs on Region B

To demonstrate the proliferation of cells, OD values were used to test the change of cells' number. As shown in Fig.8, the cells' number kept increasing after seeding, reached a peak at the 9th day, then gradually reached saturated and began to decrease afterward. Comparing the OD values of Region A with Region B at the first day, it showed that PL could promote the initial adhesion of ASCs. During days 3~7, cells in the logarithmic growth phase, the ASCs proliferation rate in the Region B was significantly higher than that in Region A.

ASCs in different region had different proliferation rate, it was influenced by the properties of biomaterials, including composition, surface energy and electron charges. Therefore the method to the realization of cell directional migration and accumulation by modifying and setting the material gradient is feasible.

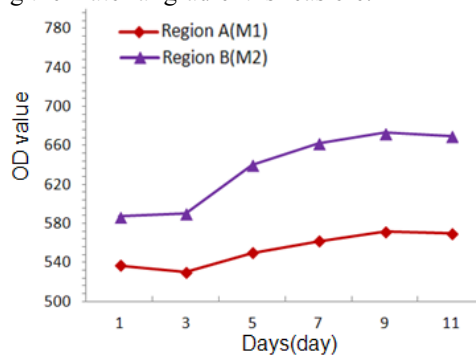


Figure 8. Proliferation of ASCs cultured on different region determined by DNA assay using Hoechst 33258

3. Conclusion

In this work, preparing composite gradient scaffold including physical gradient and material gradient has been initially realized and improvement of the mechanical properties and some biological parameters can also be realized through optimizing scaffold architecture and the scaffold material. Therefore this method is feasible for preparing biomimetic bone scaffold, and can provide a new technique for constructing complicated tissues and organs in vitro. However, until now this research remain in the experimental stage, and the methods, materials and structure features used in the research are not the most ideal ones, and have much room for further improvement and perfection.

Acknowledgements

This study is financially supported by National Natural Science Foundation of China (51375292), National Youth Foundation of China (51105239).

References

- [1] Howard D, Buttery LD, Shakesheff KM, et al, Tissue engineering: strategies, stem cells and scaffolds, *J. Anat.* (2008) 66-72.
- [2] Yu G, Ji J, Zhu H, et al. Poly(D,L-lactic acid)-block-(ligand-tethered poly(ethylene glycol)) copolymers as surface additives for promoting chondrocyte attachment and growth, *J. Biomed Mater Res B Appl Biomater.*(2006) 64-75.
- [3] Higuchi A, Ling QD, Chang Y, et al. Physical cues of biomaterials guide stem cell differentiation fate, *J. Chem Rev.* (2013) 3297-3327.
- [4] Fedorovich NE, Kuipers E, Gawlitta D, et al. Scaffold Porosity and Oxygenation of Printed Hydrogel Constructs Affect Functionality of Embedded Osteogenic Progenitors, *J. Tissue Engineering: Part A* (2011) 2473-2486.
- [5] Brennan M Bailey, Lindsay N Nail, Melissa A Grunlan, et al. Continuous gradient scaffolds for rapid screening of cell-material interactions and interfacial tissue regeneration, *Acta Biomaterialia* (2013) 8254-8261.
- [6] Zhang Jian-ming, Zhang Xi-zheng, LiRui-xin,et al, Preparation of tissue engineering scaffolds using rapid prototyping, *J. Chinese Journal of Tissue Engineering Research* (2013) 1435-1440.
- [7] Andreas Pfister, Rüdiger Landers, Andres Laib, et al, Biofunctional rapid prototyping for tissue-engineering applications: 3D biplotting versus 3D printing, *J. J Polym Sci Part A: Polym Chem* (2004) 624-638.
- [8] Susmita Bose and Sahar Vahabzadeh. Bone tissue engineering using 3D printing, *J. Materials Today* (2013) 496-504.
- [9] Jorge M. Sobral, Sofia G. Caridade, Rui A. Sousa. Three-dimensional plotted scaffolds with controlled pore size gradients: Effect of scaffold geometry on mechanical performance and cell seeding efficiency, *J. Acta Biomaterialia* (2011) 1009-1018.
- [10] SeungHyun Ahn, HyeongJin Lee, Lawrence J. Bonassar. Cells (MC3T3-E1)-Laden Alginate Scaffolds Fabricated by a Modified Solid-Freeform Fabrication Process Supplemented with an Aerosol Spraying, *J. Biomacromolecules* (2012) 2997-3003
- [11] Chih-Hui Yang, Keng-Shiang Huang, Chih-Yu Wang, et al, Microfluidic-assisted synthesis of hemispherical and discoidal chitosan microparticles at an oil/water interface, *J. Electrophoresis* (2012) 3173-3180.
- [12] He Shulan, Yin Yuji, Zhang Min,et al, Research Advances on Sodium Alginate Hydrogels for Tissue Engineering, *J. Chemical industry and engineering progress* (2004) 1174-1177.
- [13] Andrew Darling, Lauren Shor, Saif Khalil, et al, Multi-Material Scaffolds for Tissue Engineering, *J. Macromol. Symp* (2005) 345-355.
- [14] GONG Haipeng, ZHONG Yinghui, GONG Yandao, et al, The influence of chitosan and polylysine related materials on nerve cells, *J. Biological Physics* (2000) 553-559.

- [15] Mao Xueli, Ling Junqi, Xiao Yin, et al. Modified poly (L-lactic acid)-poly (L-lysine) polymer induces bone marrow stromal cells initial adhesion, *J. Journal of Clinical Rehabilitative Tissue Engineering Research* (2011) 7100-7104.
- [16] Peng Ying, Tian Jing. Surface modification of bone repair material and osteogenesis, *J. Int J orthop.* (2012) 99-102.
- [17] Wu Jindan, *Construction of Grafting Density Gradient Surfaces for the Manipulation of Cell Migration*, Ph.D. Dissertation, Zhe Jiang University, 2012.
- [18] Oju Jeon, Daniel S Alt, Stephen W Linderman, et al. Biochemical and Physical Signal Gradients in Hydrogels to Control Stem Cell Behavior, *J. Adv. Mater.* (2013) 6366–6372.
- [19] Y. X. Wang, J. L. Robertson, W. B. Spillman et al, Effects of the chemical structure and the surface properties of polymeric biomaterials on their biocompatibility, *J. Pharm Res* (2004) 1362-1373.
- [20] K.Tsuchiya, G.P Chen, T Ushida, et al, Effects of cell adhesion molecules on adhesion of chondrocytes, ligament cells and mesenchymal stem cells, *J. Mater.Sci.Eng: C*, (2001) 79-82.